Experimental investigation of the heat and mass transfer in a centrifugal fluidized bed dryer

M.H. Shi*, H. Wang, Y.L. Hao

Department of Power Engineering, Southeast University, Nanjing 210096, China

Abstract

An experimental study of the heat and mass transfer characteristics of wet material in a drying process in a centrifugal fluidized bed (CFB) dryer was carried out. The rotating speed ranged from 300 to 500 rpm. Wet sand, glass beads and sliced food products were used as the testing materials. The gas temperature and the wet bulb temperature at the inlet and outlet, as well as the bed temperature, were measured. The moisture contents were determined instantaneously by the mass balance method in the gas phase. Influences of the superficial gas velocity, particle diameter and shape, bed thickness, rotating speed of the bed and initial moisture on the drying characteristics were examined. One empirical correlation which can be used to calculate the heat transfer coefficients of the gas particles in the centrifugal fluidized dryer were obtained. © 2000 Elsevier Science S.A. All rights reserved.

Keywords: Drying; Heat and mass transfer; Centrifugal fluidized bed

1. Introduction

Centrifugal fluidized bed (CFB) drying is a new technology in which the wet material undergoes a highly enhanced heat and mass transfer process in a centrifugal force field by rotating the bed. The bed essentially is a cylindrical basket rotating around its symmetric axis with a porous cylindrical wall. The drying material is introduced into the basket and forced to form an annular layer at the circumference of the basket due to the large centrifugal forces produced by rotation. The gas is injected inward through the porous cylindrical wall and the bed begins to fluidize when the forces exerted on the material by the fluidizing medium balance the centrifugal forces. Instead of having a fixed gravitational field as in a vertical bed, the body force in a centrifugal bed becomes an adjustable parameter that can be determined by the rotation speed and the basket radius. Minimum fluidization can, in principle, be achieved at any gas flow rate by changing the rotating speed of the bed. By use of a strong centrifugal field much greater than gravity, the bed is able to withstand a large gas flow rate without the formation of large bubbles. Thus, the gas–solid contact at a high gas flow rate is improved and heat and mass transfer can be achieved during the drying process. For this reason, the CFB dryer has received much attention in the drying industry.

Only a few research works dealing with drying in the CFB could be found in the literature. Lazar and Farkas [1,2] and Brown [3] have conducted the drying process in a CFB for sliced fruits and vegetables, while Carlson [4] investigated the drying of rice in the CFB. These research works are very instructive, but they are mainly focused on the possibility of an industrial application for CFB. The flow behaviour and drying characteristics in the CFB are very complicated and still unclear. A knowledge of heat transfer from the gas to the material is desirable in order to estimate the material surface temperature from the measured temperature of the gas. A quantitative knowledge of the heat transfer characteristics of CFBs is therefore necessary for design purposes [5].

In this paper, an experimental study of the flow behaviour and gas–solid heat and mass transfer characteristics in a CFB dryer was performed and the main factors which influence the drying process were examined and discussed.

2. Experimental apparatus

A schematic diagram of the experimental apparatus is shown in Fig. 1. A cylindrical basket rotated about a horizontal axis is mounted in a sealed cylindrical casing. The basket is 200 mm in diameter and 80 mm in width. The side surface of the basket contains 3 mm diameter holes which serve as a gas distributor, with an open area of 22.7%. A

---

* Corresponding author.

Fig. 2. A differential section in a centrifugal fluidized bed.

The water balance in the time interval from t_j to t_{j+1} is

$$G \int_{t_j}^{t_{j+1}} (H_{\text{out}} - H_{\text{in}}) \, \mathrm{d}t = -M_s \int_{x_j}^{x_{j+1}} \mathrm{d}x \tag{1}$$

and thus, the moisture content of the test material at time t_{j+1} is

$$x_{j+1} = x_j - \frac{G}{M_s} \int_{t_j}^{t_{j+1}} (H_{\text{out}} + H_{\text{in}}) \, \mathrm{d}t \tag{2}$$

By using the drying weight method for a test material sample to obtain the initial moisture content, we can obtain the moisture content variation with time, and thus, the drying rate can be calculated as
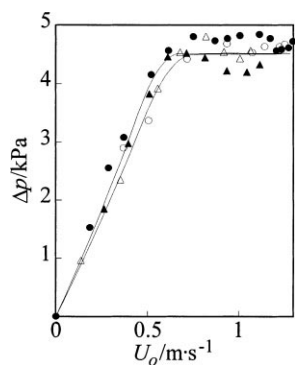
Fig. 1. Experimental apparatus.

200 mesh stainless steel screen is coated on the inside surface to prevent the bed material from leaching out. There is one hole 80 mm in diameter located at the centre of the end wall of the basket to exit the gas. A variable speed motor is used to rotate this basket by means of a shaft connected to the other end wall of the basket. Rotational speeds of the motor are measured using an LZ-45 revolution counter.

Air is blown in from a blower. The mass flow rates of air are measured using an orifice meter. Air is heated using an electric heater. A tee valve is used to control the flow direction. After the air temperature is steady at the desired value (about 100°C), the drying experiments begin by turning the tee valve on; the hot air flows through the distributor to the bed and then is exhausted into the atmosphere. The pressure drop is measured by a U-shaped pressure gauge. A pressure probe is stretched into the basket along the centreline 10 mm away from the end wall of the basket. Experiments are also conducted without bed material to obtain the pressure differentials across the distributor under the same operating conditions. The pressure drop through the bed is then calculated by

$$\Delta p_{\text{Bed}} = \Delta p_{\text{Total}} - \Delta p_{\text{Distributor}}$$

The inlet gas temperature, the outlet gas temperature and the bed temperatures at various positions versus time are measured using the bare thermocouple probes, and the data are recorded by a 3497A data acquisition/control unit. Moisture contents of the test material during the drying process are measured by the moisture balance method in the gas phase, i.e. by measuring the inlet and outlet wettabilities in the gas phase with wet and dry bulb thermometers.

Fig. 3. The fluidized curve of sand in the CFB (d_p=0.245 mm, n=400 rpm). Material (up/down): (▲/□) sand; (●/○) glass beads.

Fig. 4. The fluidized curves for materials with different shapes: (△) pieces of potato 10 mm×10 mm×1.5 mm, n=300 rpm; (□) blocks of potato 5 mm×5 mm×5 mm, n=300 rpm; (○) block of potato 5 mm×5 mm× 5 mm, n=250 rpm.

speeds during the drying tests. In the initial fluidizing stage, the pressure drop increases linearly with increasing gas velocity. After reaching the critical point, the pressure drop will be almost constant. However, different results are observed for sliced and block materials. The pressure drop curve has a maximum value that corresponds with the critical fluidization point as shown in Fig. 4. In the initial fluidizing stage, the pressure drop increases slowly with increasing gas velocity. After reaching the critical point, the pressure drop will decrease with increasing gas velocity. This is because the self-lock phenomenon of the sliced material under a centrifugal force field will be weakened and because the bed becomes uniform. This causes a decrease in the flow resistance. Decreasing the bed rotating speed would decrease the bed pressure drop and the critical gas velocity remarkably, as also shown in Fig. 4. This is because decrease in the bed rotating speed would weaken the centrifugal force field and cause the flow resistance to decrease. It can be seen from Fig. 4 that the critical fluidized velocity for pieces of potato is somewhat smaller than that of blocks of potato owing to the
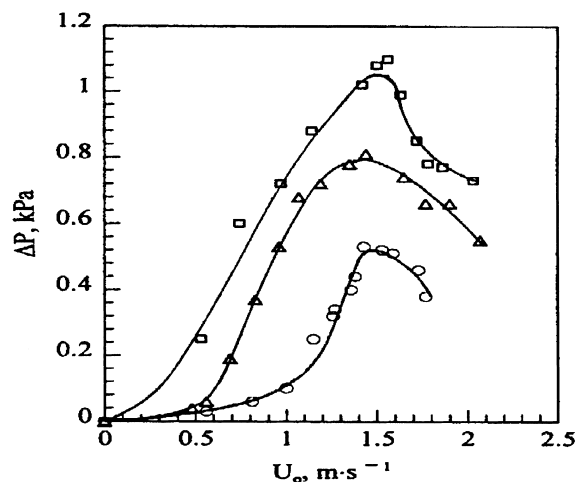
larger upwind surface area for pieces of material. Furthermore, pressure drop of the piece material bed is also smaller than that of the block material bed because the pieces of material show better fluidization character in the CFB. The initial fluidizing relationships obtained from the theoretical model for granular material [6] do not fit the sliced material. The initial fluidizing conditions for the sliced material with different shapes should be determined experimentally and individually.

3.2. Drying curves

Typical gas temperature and bed temperature curves as well as the drying curve of wet sand in the intermittent drying process are shown in Fig. 5. This shows that the drying
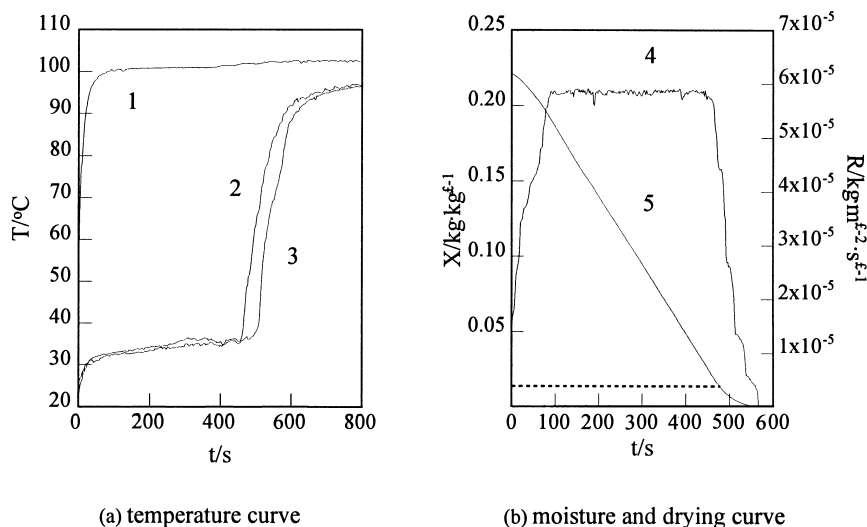

(a) temperature curve

(b) moisture and drying curve

Fig. 5. Intermittent drying curve in the CFB (sand, d_p=0.411 mm, M=2.48 kg, ω=41.9 rad s^{-1}, U_0=1.71 m s^{-1}, H_{in}=0.016 kg kg^{-1}): (1) $T_{g,in}$; (2) $T_{g,out}$; (3) T_b; (4) R; (5) x.
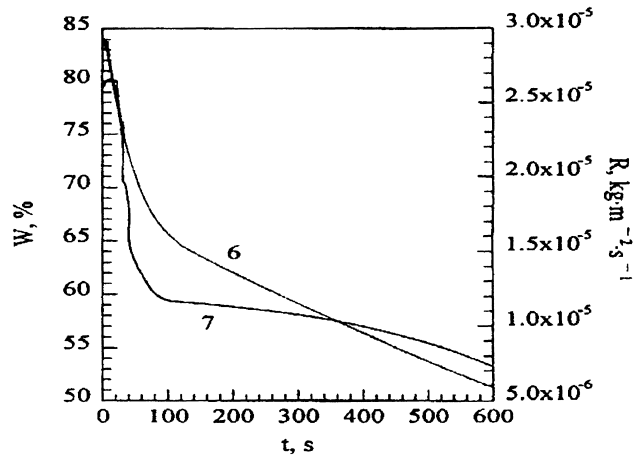
Fig. 6. Variations in the moisture content (Curve 6) and drying rate (Curve 7) for sliced potato.

characteristics of materials like sand in the CFB, in which the moisture content is mainly surface water, are the same as in an ordinary dryer, i.e. the whole drying process can be divided into three stages. At a short initial stage, the material is preheated and the drying rate increases rapidly; the bed temperature is increased to a stable value. The second stage is a constant drying rate stage in which the heat transferred from gas to material is expended totally for evaporation of the surface water of the material. The material temperature remains constant and the drying rate is also constant. The last stage is called the falling rate stage in which the material temperature increases gradually and the drying rate decreases until the end of drying.

The drying behaviour for sliced food products in the CFB is somewhat different from sand as shown in Fig. 6. It is obvious that sliced potato has a drying character in the CFB that is basically similar to that in the conventional drying process. In the beginning, there is a short initial period. In this period, the bed material is preheated; the bed temperature approaches a stable value quickly and the drying rate increases very rapidly. This initial period is followed by a period of a constant rate of drying. In the constant rate period, the surface of the test material is covered with a thin water film. The heat transferred from the gas flow to the material is used completely to evaporate the moisture, so that the temperature of the sliced material remains at an equilibrium temperature and the drying rate is at the maximum value. As the main moisture content in potato is cell water, the constant rate period is very short. The most important drying process is completed in the falling rate period. In the falling rate period, the dry layer appears and gradually becomes thicker near the surface owing to the larger transport resistance of the inner moisture outward. This causes the heat transfer resistance to increase and the drying rate to decrease rapidly in the first stage. After the dried layer's temperature has increased to a certain value, a slow decrease in the drying rate occurs. This indicates that the falling rate

period for the sliced potato in the CFB dryer can be divided into two different stages. This is significant for engineering design and operation.

The experimental results show that the pieces of potato in the drying process have a larger drying rate and a shorter drying time than blocks of potato in the CFB. This is because the transport distance of moisture from the inner cell to the outer evaporating surface in the pieces of material is much shorter than in the blocks of material; in particular, the second stage of the falling rate period is shorter for the pieces of material during the drying process. In general, because the sliced material could be fluidized and mixed very well in the CFB, the drying time is extremely short. For example, the drying time is 15 times shorter in the CFB for sliced potato than in the tunnel dryer and five times shorter than in the conventional fluidized dryer.

3.3. Influences of the operational parameters

3.3.1. Superficial gas velocity

It is obvious that an increase in the superficial velocity would increase the degree of fluidization, and thus, the heat and mass transfer between the gas and the solid phase would be greatly enhanced. This causes the drying rate to be larger and the drying time to be shorter, as shown in Fig. 7. The critical moisture content would be increased with increasing gas velocity, indicated by the broken line in Fig. 7. For food material, the experimental results show that the drying rate in the constant rate period and the first stage of the falling rate period would increase with increasing gas velocity in the low gas velocity range. Thus, the total drying time would be decreased. However, when the gas velocity is increased to a certain value, the constant rate period would disappear, the first stage of the falling rate period
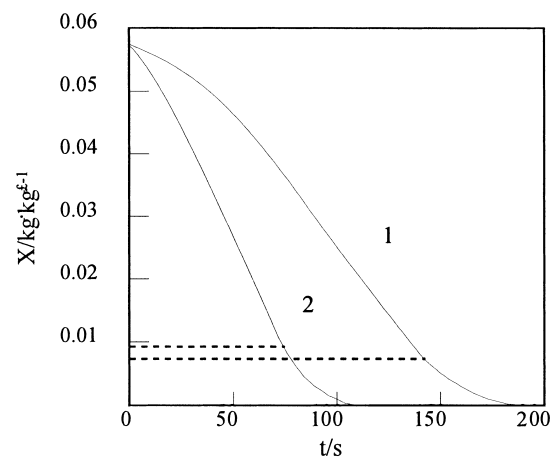

Fig. 7. The influence of superficial velocity on the moisture content (d_p=0.411 mm, M=2.50 kg, ω=41.9 rad s^{-1}, H_{in}=0.016 kg kg^{-1}): (1) U_0=1.66 m s^{-1}; (2) U_0=2.17 m s^{-1}.

would decrease and the second stage would increase. The total drying time would remain unchanged; this is because the main water content in potato is the inner cell water and the main drying process is in the second stage of the falling rate period. With an increase in the inlet gas temperature, the drying rates in all drying periods increase and the total drying time will decrease. However, the increase in gas temperature would be limited by the quality of the dried food products. In our test, the best inlet gas temperature is about 100–110°C.

The experimental results also show that pieces of radish with given dimensions show a larger drying rate than pieces of potato under the same operating conditions. This is because the microstructures of the test examples indicate that radish has a larger cell structure with a more regular arrangement than potato, and furthermore, the liquid in the radish cell is less viscous; these structural characteristics make radish easy to dry.

3.3.2. Rotating speed

At the same gas velocity, a decrease in the bed rotating speed will reduce the centrifugal force acting on the material and increase the fluidized degree of the material; this causes the heat and mass transfer between the gas and the solid phase to increase. Thus, when decreasing the bed rotating speed, the drying rate will be larger, as shown in Fig. 8, and the drying process will be much more uniform over the whole bed. This means that, for a given material drying in the CFB, the bed rotating speed should be as low as possible until the fluidization state cannot be maintained. When it is desired that the drying process be enhanced by increasing the gas velocity in the CFB dryer, the bed rotating speed must be increased simultaneously to avoid the drying material from blowing out of the bed. Theoretically, the bed can be operated in the optimum fluidized condition at any gas velocity by regulating the bed rotating speed in the CFB.
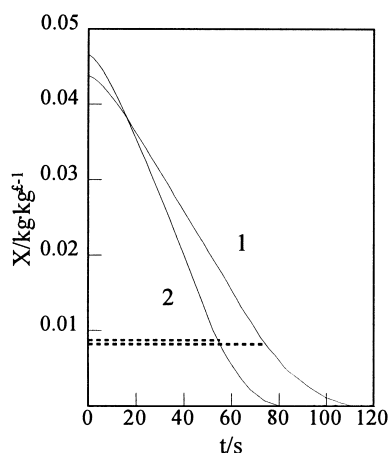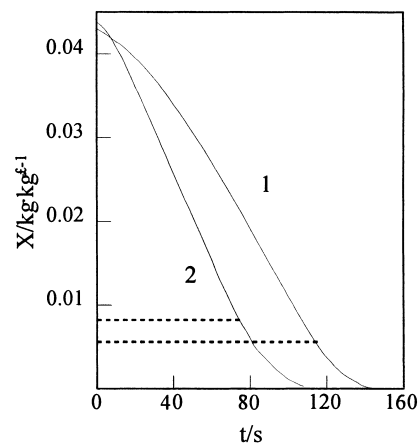

Fig. 9. The influence of particle diameter ($M=2.4$ kg, $\omega=41.9$ rad s^{-1}, $U_0=1.43$ m s^{-1}, $H_{in}=0.0123$ kg kg^{-1}): (1) $d_p=0.245$ mm; (2) $d_p=0.411$ mm.

3.3.3. Partial diameter

Fig. 9 shows the influence of particle diameter on the drying behaviour in the CFB. It is clear that, owing to the larger slip velocity between gas and solid particles for particles with larger diameters, the heat and mass transfer in the drying process would be enhanced; thus, the drying rate in the CFB would increase with increasing particle diameter as shown in Fig. 9. However, with increasing material dimensions, the internal heat and mass transfer resistance would be increased; thus, for a given material to be dried, it is important to determine the optimum material dimensions in the drying process under certain given operating conditions.

3.3.4. Bed thickness

Fig. 10 shows the effect of initial bed thickness on the drying process. It can be seen that, with increasing bed thickness, the drying rate would be decreased; this is because the heat and mass transfer driving force between the gas and the solid phase is larger in the shallow bed situation.
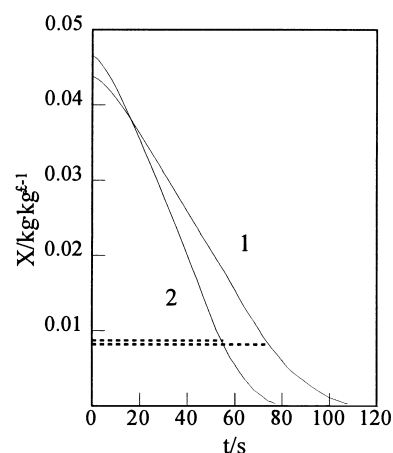

Fig. 8. The influence of rotating speed ($d_p=0.411$ mm, $M=2.41$ kg, $U_0=1.43$ m s^{-1}, $H_{in}=0.0123$ kg kg^{-1}): (1) $\omega=52.4$ rad s^{-1}; (2) $\omega=41.9$ rad s^{-1}.

Fig. 10. The influence of bed thickness ($d_p=0.411$ mm, $\omega=41.9$ rad s^{-1}, $U_0=1.43$ m s^{-1}, $H_{in}=0.0123$ kg kg^{-1}): (1) $L_0=30$ mm; (2) $L_0=20$ mm.
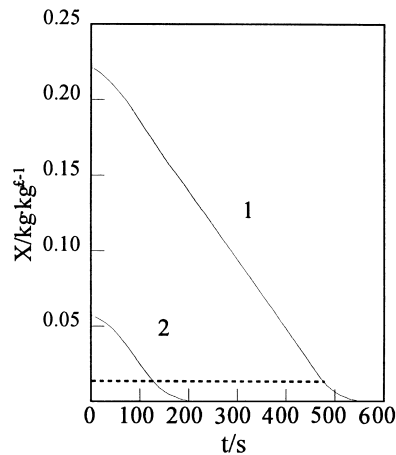
Fig. 11. The initial moisture content (d_p=0.411 mm, M=2.48 kg, ω=41.9 rad s^{-1}, U_0=1.71 m s^{-1}, H_{in}=0.016 kg kg^{-1}): (1) x_0=0.221 kg kg^{-1}; (2) x_0=0.0574 kg kg^{-1}.

3.3.5. The effect of initial moisture content

It is obvious that a material with a large initial moisture content has a much longer drying time (Fig. 11), but the drying characteristics are the same. The only difference is in the duration of the constant rate stage.

3.4. The heat transfer correlation

Sixty-five experimental runs of wet sand and glass beads were carried out under the conditions of a static bed thickness range from 10 to 30 mm, Reynolds number from 5.47 to 35.3 and centrifugal force from 10.08 to 28 multiples of gravity. The heat transfer coefficients were converted into Nusselt numbers using the mean diameter and the thermal conductivity of air at the average temperature.

The dimensionless correlation of heat transfer between gas and particles in the CFB during drying is obtained by use of a regression procedure. The exponent of the diffusivity ratio (Prandtl number) has been assumed to be 1/3; thus,
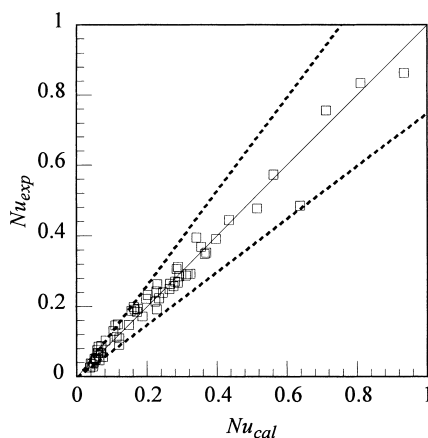

Fig. 12. Comparison of experimental and calculated results.

$$\mathrm{Nu} = 5.33 \times 10^{-5}\, \mathrm{Pr}^{1/3}\, \mathrm{Re}^{1.59}\, F_c^{-0.48}$$
$$\times \left(\frac{L_0}{d_p}\right)^{-0.21} \left(\frac{\rho_s}{\rho_g}\right)^{0.79} \tag{7}$$

The suitable parameter ranges for the above two correlations are Re=5.0–42.0, F_c=10.0–28.0. In Eq. (7), the Nusselt number is defined as Nu=hd_p/λ; the Reynolds number is Re=$\rho_g U_0 d_p/\mu$; the Prandtl number is Pr=$c_{pg}\mu/\lambda$; and then, dimensionless centrifugal force is defined as $F_c = r_0\omega^2/g$.

Comparison of the experimental heat transfer data with the values calculated by Eq. (7) is shown in Fig. 12. The deviation for all test data obtained in this work is within ±25%.

4. Conclusions

1. The CFB may be operated in the packed bed, incipient fluidization or fluidized bed states at a given gas velocity. Steady fluidized states can be maintained at large gas flow rates by using a strong centrifugal force field.
2. There is no evident 'active region' near the distributor of the CFB. The gas–solid heat transfer comes under the influence of the superficial gas velocity, particle diameter, particle shape factor, particle density, bed thickness and rotational speed of the bed.
3. The drying process can be divided into three stages in the CFB dryer and the drying rate increases with increasing superficial gas velocity and particle diameter and decreasing bed rotating speed and initial bed thickness.
4. Sliced food products can be fluidized and mixed very well in the CFB. The pressure drop curve has a maximum value and the critical fluidized parameters vary with the shape and dimensions of the drying products and the material itself, as well as the operating conditions.
5. Sliced food products can be dried very well and efficiently. The main process of drying is within the falling rate period; the drying rate depends on the shape, dimensions and material of the drying products, as well as the operating conditions.

5. Nomenclature

a	particle surface per unit volume (m^2 m^{-3})
c_{pg}, c_{ps}	specific heat of gas or solid (J kg^{-1} °C^{-1})
d_p	mean particle diameter (m)
D_{AB}	molecule diffusivity (m^2 s^{-1})
F_c	dimensionless centrifugal force, $r_0\omega^2/g$
G	mass flow rate of gas (kg s^{-1})
h	heat transfer coefficient (W m^{-2} °C^{-1})
H	width of bed (m); wettability of gas (kg kg^{-1})
L_0	fixed bed thickness (m)
M	weight of dried material (kg)

n rotating speed of the bed (rpm)
Nu   Nusselt number, hd_p/λ
ΔP pressure drop (kPa)
Pr   Prandtl number, $c_{pg}\mu/\lambda$
R drying rate (kg m^{-2} s^{-1})
Re   Reynolds number, $U_0 d_p/\nu$
T temperature (°C)
U_0 superficial gas velocity (m s^{-1})
x moisture content (kg kg^{-1})

Greek letters

ε porosity
λ heat conductivity (W m^{-1} °C^{-1})
μ viscosity of gas (kg m^{-1} s^{-1})
ν kinematic viscosity of gas (m^2 s^{-1})
ρ_g, ρ_s density of gas or solid (kg m^{-3})
ϕ_s sphericity
ω angular velocity (rad s^{-1})

Acknowledgements

References

[1] M.E. Lazar, D.F. Farkas, The centrifugal fluidized bed. 2. Drying studies on piece form foods, J. Food Sci. 36 (1971) 315–319.

[2] M.E. Lazar, D.F. Farkas, J. Food Sci. 44 (1979) 242–246.

[3] G.E. Brown, D.F. Farkas, Centrifugal fluidized bed, Food Technol. 26 (12) (1972) 23–30.

[4] R.A. Carlson, R.L. Roberts, D.F. Farkas, Preparation of quick cooking rice products using a centrifugal fluidized bed, J. Food Sci. 41 (1976) 1177–1179.

[5] D.F. Hanni, D.F. Farkas, G.E. Brown, Design and operating parameters for a continuous centrifugal fluidized bed drier, J. Food Sci. 41 (1976) 1172–1176.

[6] C.I. Metcalfe, J.R. Howard, Fluidization, Cambridge University Press, Cambridge, 1978, pp. 276–327.